J Fluoresc (2012) 22:1431–1439
DOI 10.1007/s10895-012-1080-y

ORIGINAL PAPER

Spectroscopic Study on the Effect of Imidazophenazine Tethered to 5′-End of Pentadecathymidilate on Stability of Poly(dA)·$(dT)_{15}$ Duplex

Olga Ryazanova · Larysa Dubey · Igor Dubey · Victor Zozulya

Received: 24 October 2011 / Accepted: 20 June 2012 / Published online: 1 July 2012

Abstract The effect of imidazo[4,5-d]phenazine (Pzn) attached to the 5′-end of $(dT)_{15}$ oligonucleotide via a flexible linker on the thermal stability of poly(dA)·$(dT)_{15}$ duplex was studied in aqueous buffered solution containing 0.1 M NaCl at the equimolar ratio of adenine and thymine bases (100 μM each) using spectroscopic techniques. Duplex formation was investigated by measuring UV absorption and fluorescence melting curves for the Pzn-modified system. Tethered phenazine derivative enhances the thermostability of poly(dA)·$(dT)_{15}$ duplex increasing the helix–to–coil transition temperature by 4.5 °C due to an intercalation of the dye chromophore between AT-base pairs. The thermodynamic parameters of the transition for non-modified and modified systems were estimated using "all–or–none" model. The modification of the $(dT)_{15}$ results in a decrease in the transition enthalpy, however, the observed gain in the Gibbs free energy of complex formation, ΔG, is provided with the corresponding decrease in entropy change. The increase of ΔG value at 37 °C in consequence of $(dT)_{15}$ modification was found to be equal to 1.3 kcal/mol per oligonucleotide strand.

Keywords Imidazophenazine · Fluorescent probe · Modified oligonucleotide · Duplex · Melting · Absorption · Fluorescence

O. Ryazanova (✉) · V. Zozulya
Department of Molecular Biophysics, B. Verkin Institute for Low Temperature Physics & Engineering of the NAS of Ukraine,
47 Lenin Ave.,
61103 Kharkov, Ukraine
e-mail: ryazanova@ilt.kharkov.ua

L. Dubey · I. Dubey
Department of Synthetic Bioregulators, Institute of Molecular Biology and Genetics of the NAS of the Ukraine,
150 Acad. Zabolotnogo str.,
03143 Kyiv, Ukraine

Introduction

During the last three decades, an elaboration of highly selective therapeutic agents based on the synthetic oligonucleotides showing anticancer, antiviral or antimicrobial activity has attracted considerable interest [1, 2]. Three main classes of such agents are known. The effect of antisense oligodeoxynucleotides (AS ODN) is based on their sequence-specific hybridization to mRNA target region and consequently on targeted inhibition of the translation that leads to the inhibition of the corresponding protein synthesis [3–6]. Reagents of the second class, triplex forming oligonucleotides (TFO), form three-helical structures with target region of double-helical DNA significantly affecting an expression of the genetic code [7, 8]. Third class, aptamers, can bind to selected proteins blocking them similarly to antibodies [1, 9].

Both the computations and empirical estimations show that the best specificity to target sequences is observed for the antisense oligonucleotides of 15–21 nucleotides in length [1]. To improve their therapeutic properties the antisense oligonucleotides can be modified in several ways. One of the most commonly used ways is the tethering of intercalative organic dye to the end of the oligonucleotide via a flexible linker [10–13]. Alternative approach consists in the direct insertion of a dye nucleoside analogue into the oligonucleotide chain instead of "native" nucleotide [14]. In both cases the conjugation of the oligonucleotide with the intercalator strengthens substantially the stability of its complex with complementary target sequence, improves the oligonucleotide transport into the cell, as well as increases its resistance to nucleases [15]. A stabilizing effect induced by the tethered dye is conditioned by the additional binding energy provided by the interaction between π-systems of nucleic bases and the chromophore itself resulting from their stacking. The value of the effect strongly depends on the

type of the intercalator, nucleotide sequence, the chemical character and length of linker, and the site of tethering [16]. The most frequently used chromophores are acridine, phenazine, ethidium, anthracene, pyrene, porphyrin and cyanine derivatives [12].

Imidazo[4,5-d]phenazine (Pzn) dye is known as the fluorescent intercalative agent possessing a planar tetracyclic chromophore with extended π-system [17], whose spectral properties have been reported earlier [18, 19]. In our previous works an effect of its nucleoside analogue, imidazo[4,5-d] phenazine N1-β-D-ribofuranoside (PznRib), covalently attached to the 3′-end of oligothymidylate on the thermostability of the duplexes and triplexes formed with complementary deoxyribooligo- and polynucleotides $(dA)_{15}\cdot(dT)_{10}$PznRib, $(dA)_{15}\cdot 2(dT)_{10}$PznRib, poly(dA)·poly(dT)·$(dT)_{10}$PznRib [20], as well as with mixed ribo/deoxyribonucleotide systems poly(rA)·$(dT)_{10}$Pzn [21] and poly(rA)·$(dT)_{14}$Pzn [22] were investigated. Substantial enhancement of complex thermostability was revealed depending on the length and the type of constituent biopolymers.

In the present work the effects of imidazo[4,5-d]phenazine (Pzn) attached to $(dT)_{15}$ in another way, via a flexible linker based on hexamethylenediamine, on the thermal stability of poly(dA)·$(dT)_{15}$ duplex and on the thermodynamic parameters of helix-to-coil transition have been investigated using spectroscopic techniques.

Materials and Methods

Materials

Sodium salt of poly(dA) from Sigma Chemical Co. was used without additional purification. Synthesis of $(dT)_{15}$ oligonucleotide was performed on Applied Biosystems 381A DNA synthesizer by a standard solid phase phosphoranidite method. 5′-Aminohexyl group was introduced by the modified carbonyldiimidazole method [23]. After ammonia treatment the crude oligomer was desalted by gel filtration on PD-10 column (Pharmacia, Sweden) and used for the coupling reaction without further purification. Amino-modified $(dT)_{15}$ was conjugated to N1-carboxyethyl imidazo[4,5-d]phenazine [24] using BOP-HOBT coupling method [25]. The product was purified by standard electrophoresis in 20 % denaturing polyacrylamide gel (isolated yield 25 %). Molecular structure of the obtained pentadecathymidylate-imidazophenazine conjugate, $(dT)_{15}$Pzn, is presented in Fig. 1. For all experiments 2.5 mM sodium cacodylate buffer (pH 6.9) containing 0.5 mM EDTA and 0.1 M NaCl was used as a solvent. It was prepared using deionized redistilled water.

Oligonucleotide and polynucleotide concentrations were determined by UV spectrophotometry using the

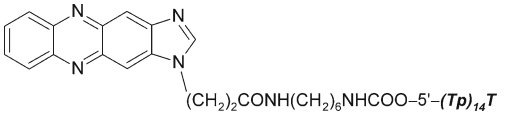

Fig. 1 Molecular structure of imidazophenazine-pentadecathymidilate conjugate

following extinction coefficients (per mole of nucleotides): $\varepsilon_{257}=8600\ M^{-1}\ cm^{-1}$ for poly(dA) [26], $\varepsilon_{266}=8600\ M^{-1}\ cm^{-1}$ for $(dT)_{15}$ [27] at 20–23 °C. The strand concentration of $(dT)_{15}$Pzn conjugate was calculated from long-wave absorbance of the dye moiety using $\varepsilon_{385}=16300\ M^{-1}cm^{-1}$ [19]. Formation of the double-helical structure by $(dT)_{15}$ or $(dT)_{15}$Pzn with complementary poly(dA) strand was studied in the mixture of constituent polymers under 1:1 ratio of adenine and thymine bases, 100 μM each.

UV–Vis Spectroscopy and Fluorescence Experiments

Electronic absorption spectra were measured in quartz cells on SPECORD UV/VIS spectrophotometer (Carl Zeiss, Jena, Germany). Fluorescent measurements were carried out on laboratory spectrofluorimeter by the method of photon counting [28]. The fluorescence was excited by the stabilized linearly polarized radiation of a halogen lamp, at $\lambda_{ex}=450$ nm. The emission was observed at an angle of 90° from the excitation beam. The polarization degree of fluorescence, p, has been determined from the equation [29]:

$$p = \frac{I_{II} - I_{\perp}}{I_{II} + I_{\perp}} \quad (1)$$

where I_{II} and $I_{\perp}$ are intensities of the emitted light, which are polarized parallel and perpendicular to the polarization direction of exciting light, respectively. The spectroscopic experiments were carried out at room temperature from 20 to 22 °C.

Melting Experiments

Absorption melting profiles were obtained by monitoring the thermally induced changes in absorbance at 260 nm and 387 nm. The cell was inserted into a copper holder which temperature was varied using the computer-operated Peltier element, the rate of heating/ cooling was 0.5 °C/min. Fluorescence melting profiles were recorded by registering the fluorescence intensity versus the temperature at 546 nm corresponding the emission maximum for the free $(dT)_{15}$Pzn, using the same cell inserted into the spectrofluorimeter. The melting curves were reproduced in repeated experiments with maximal temperature shift of ±0.2 °C.

Results and Discussion

UV–Vis Absorption and Fluorescence Spectroscopic Studies

Figure 2 shows UV–vis electronic absorption and fluorescence spectra of free $(dT)_{15}$Pzn conjugate and poly(dA)-bound one. As can be seen from the figure, the absorption spectrum of the conjugate consists of intense UV-band centered at 265 nm, less intense visible band located near 387 nm and longwave broad shoulder extending to 500 nm. It should be noted that the UV-band is a superposition of the two bands belonging to imidazophenazine (maximum at 262 nm) and oligothymidilate (maximum at 266 nm) moieties, whereas visible absorption spectrum is originated from the phenazine moiety alone [19]. The fluorescence spectrum of $(dT)_{15}$Pzn represents a broad structureless band centered at 546 nm. The fluorescence polarization degree, *p*, measured at the emission band maximum, was found to be equal to ~0.02. The tethering of the imidazophenazine to the end of the oligonucleotide results in the 16 nm shift of its fluorescent band maximum towards shorter wavelengths in comparison with that for the free dye, whereas corresponding red shifts of the absorption bands are only 2.5–3 nm (Table 1). These spectral changes are obviously caused by the π-π stacking interaction between aromatic systems of imidazophenazine and thymine bases [21, 30].

The binding of the conjugate to poly(dA) is accompanied by substantial absorption hypochromism (nearly 30 % for UV absorption band and 9 % for visible one), 2.5-fold fluorescence quenching and substantial increase in the fluorescence polarization degree. The small opposite shifts of the dye longwave absorption and fluorescence bands were observed. So, poly(dA)·$(dT)_{15}$Pzn visible absorption band turned out to be 3 nm red shifted in comparison with that for the conjugate alone, whereas the fluorescence band was 4 nm blue shifted under the complex formation (Table 1). These spectral changes result from Pzn moiety intercalation between dA·dT base pairs upon complex formation.

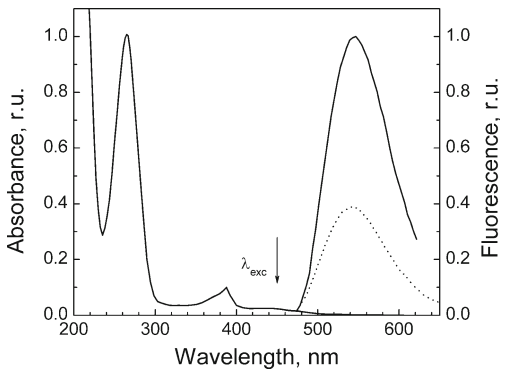

Fig. 2 Normalized absorption (left) and fluorescence (right) spectra of $(dT)_{15}$Pzn conjugate (——) and poly(dA) $(dT)_{15}$Pzn duplex (·····) measured in 2.5 mM cacodylate buffer (pH 6.9) with 0.5 mM EDTA in the presence of 0.1 M NaCl. The polymer concentration is 16 μM (in the strands). The wavelength of fluorescence excitation is λ_{exc}=450 nm

UV Absorption Melting Studies

Figure 3 represents UV absorption melting profiles for the constituent biopolymers $(dT)_{15}$ oligomer, $(dT)_{15}$Pzn conjugate and poly(dA) polynucleotide. To compare the relative changes in their absorbencies under the heating up to the temperature where the complete dissociation of the investigated duplex structures into single strands has reached, the data points were normalized by their own absorbance values at 65 °C. The independence of $(dT)_{15}$ absorption on the temperature evidences its totally disordered structure. While 2.5 % absorption increase observed during the $(dT)_{15}$Pzn melting (Fig. 3) can be conditioned by the behavior of phenazine moiety, namely by the violation of the stacking between the dye chromophore and adjacent thymine base. As for poly(dA) polynucleotide, it is well known that in neutral aqueous solutions this molecule takes the single stranded helix conformation where the base stacking occurs. Just a disruption of its secondary structure under the heating induces the absorption increase (Fig. 3). Presented dependencies have been used subsequently under the construction of upper baselines to calculate the helix-to-coil transition curve from absorption data.

Figure 4 shows melting profiles for poly(dA)·$(dT)_{15}$Pzn registered in UV and visible ranges, namely, near the polynucleotide moiety absorption maximum at 260 mn and near the dye one at 387 nm. From this figure the value of absorption hypochromism caused by the duplex formation can be clearly determined. They are 30 % for UV absorption band maximum near 260 nm and 9 % for visible band near 387 nm.

Figure 5 shows a comparison of absorption melting profiles for poly(dA) $(dT)_{15}$Pzn and poly(dA) $(dT)_{15}$ recorded under the same experimental conditions at 260 nm and converted to fraction absorbance change defined as $(A_T-A_{LT})/(A_{HT}-A_{LT})$, where A_T is the absorbance at some temperature, A_{LT} is the absorbance at the low temperature extreme investigated, and A_{HT} at the high temperature extreme investigated [31]. No a significant hysteresis was observed upon the heating and cooling of the samples (not shown). Melting curves were reproduced in repeated experiments with maximal temperature shift of ±0.2 °C. Also the normalized temperature dependence of calculated sum of absorbencies for separate constituent polymers, poly(dA) with $(dT)_{15}$ and with $(dT)_{15}$Pzn, is presented in Fig. 5. The data has been used further as upper baselines for the data processing. As can be seen from the figure, the attachment of the phenazine dye to the 5′-end of $(dT)_{15}$ oligonucleotide

Table 1 Spectral properties of Pzn and $(dT)_{15}$ alone, $(dT)_{15}$Pzn conjugate and poly(dA)·$(dT)_{15}$Pzn duplex measured in 2.5 mM cacodylate buffer pH 6.9 containing 0.5 mM EDTA and 0.1 M NaCl. Fluorescence excitation wavelength was 450 nm

Compound	UV absorption band maximum (nm)	Visible absorption band maximum (nm)	Fluorescence band maximum (nm)	Fluorescence polarization degree
Pzn	262	385	562	0.015
$(dT)_{15}$	265	–	–	–
$(dT)_{15}$Pzn	265	387.6	546	0.02
poly(dA)·$(dT)_{15}$Pzn	260	390.6	542	0.1

strengthens the corresponding duplex increasing its melting temperature by 4.5 °C. Such effect is caused by the anchorage of the duplex by planar imidazophenazine chromophore intercalated between AT base pairs.

Fluorescent Melting Studies

Figure 6 shows fluorescence melting curves recorded for $(dT)_{15}$Pzn alone and poly(dA)+$(dT)_{15}$Pzn mixture. From the figure it is clearly seen that an increase of the temperature from 20 till 80 °C is accompanied by more than 2-fold monotonic decrease of $(dT)_{15}$Pzn fluorescence intensity. The fluorescence quenching observed for the conjugate is supposed to be conditioned by the collisions between the chromophore and thymine residues. At the same time, the melting curve recorded for poly(dA)+$(dT)_{15}$Pzn mixture have qualitatively different shape. Under the temperature below 25 °C the system exists mainly in the duplex form. Observed smooth decrease in the fluorescence intensity can be explained by the temperature induced enhancement of intraduplex chromophore collisions. It can be noted that a level of the fluorescence intensity observed for poly(dA) $(dT)_{15}$Pzn duplex within this temperature range is substantially lower than that for $(dT)_{15}$Pzn. So, 2.5-fold difference in their fluorescence levels was registered at room temperature. Such quenching of Pzn fluorescence is conditioned by the π-π interaction of this chromophore embedded into the duplex with adenines under which the photoinduced electron transfer from the adenine bases in the ground state on the dye molecule in the first excited singlet state occurs [32]. Similar phenomenon was observed earlier for $(dA)_{15}$+$(dT)_{10}$PznRib [20], poly(rA)+$(dT)_{10}$PznRib [21] and poly(rA)+$(dT)_{14}$PznRib [22] systems. In the higher temperature range corresponding properly to helix-to-coil transition a rise of the temperature is accompanied by an enhancement of the sample fluorescence due to the chromophore release. After the end of the transition a temperature dependent fluorescence quenching was observed again. In this part the melting curves recorded for poly(dA)+$(dT)_{15}$Pzn and for the $(dT)_{15}$Pzn conjugate alone are practically coincident, that evidences the complete duplex dissociation.

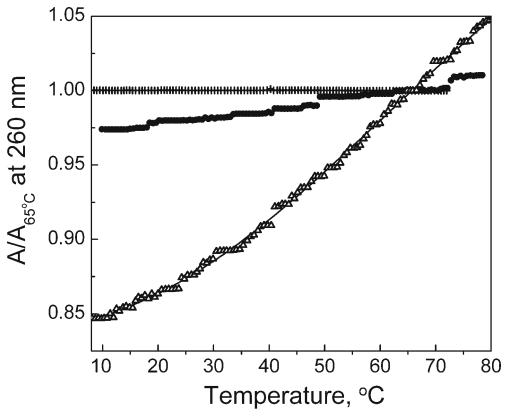

Fig. 3 Temperature dependence of absorbance at 260 mn for $(dT)_{15}$ (+), $(dT)_{15}$Pzn (●) and poly(dA) (Δ). Fifth-order polynomial fit to poly (dA) absorption melting curve is represented by the solid line. The data points of each curve were normalized to their own values at 65 °C

Thermodynamics of the Double Helix-to-Coil Transitions

To estimate the effect of the oligonucleotide modification on its hybridization properties a change in the thermodynamic parameters was evaluated. For that double helix-to-coil transition curves for poly(dA)·$(dT)_{15}$ and poly(dA)·$(dT)_{15}$Pzn systems were plotted (Fig. 7) from the absorption melting data (Fig. 5) using the standard procedure [33]. Here the fraction of paired dA·dT bases, Θ, was calculated using the equation

$$\Theta(t) = \frac{A_s - A}{A_s - A_d} \quad (2)$$

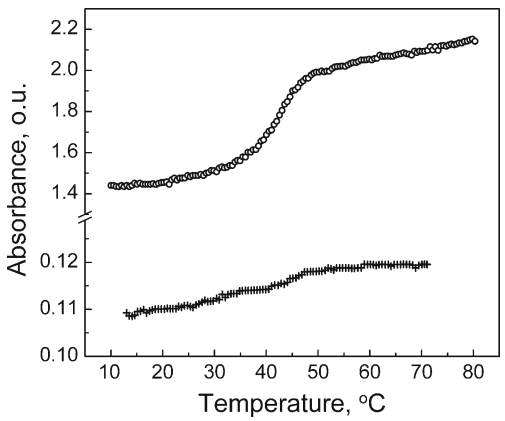

Fig. 4 Temperature dependence of poly(dA)·$(dT)_{15}$Pzn absorbance registered (A) at 260 mn (○) and (B) at 387 nm (+). Path length is 1 cm

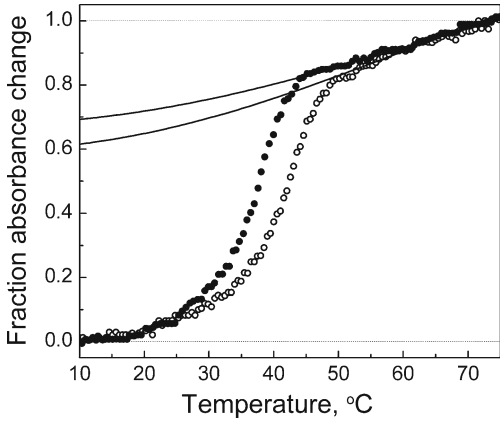

Fig. 5 Melting profiles for the poly(dA)·(dT)$_{15}$ (●) and poly(dA)·(dT)$_{15}$Pzn (○) duplexes recorded under 260 nm and converted to fraction absorbance change defined as A_T-A_{LT}/A_{HT}-A_{LT}, where A_T is the absorbance at some temperature, A_{LT} is the absorbance at the low temperature extreme investigated, and A_{HT} at the high temperature extreme investigated [31]. Measurements were carried out in 2.5 mM cacodylate buffer (pH 6.9) with 0.5 mM EDTA in the presence of 0.1 M NaCl. Adenine-to-thymine ratio was 1:1 in the both samples; the poly(dA) concentration was 100 μM in the nucleic bases. Calculated sums of absorbencies for separate constituent polymers, poly(dA) and (dT)$_{15}$ or (dT)$_{15}$Pzn, vs temperature normalized to their own values at 72 °C are shown by solid lines

where A_s is the absorption of totally denatured complex which corresponds to relative absorbance upper baseline defined by five-order polynomial fit (Fig. 5); A_d – absorption of the sample, where all constituent strands form the double helix, defined as lower steady-state levels of the relative absorption, A – the relative absorption current value.

Additionally the transition curve was plotted for poly(dA)·(dT)$_{15}$Pzn system using the fluorescence melting data. In this case the fraction of (dT)$_{15}$Pzn conjugate in the bound

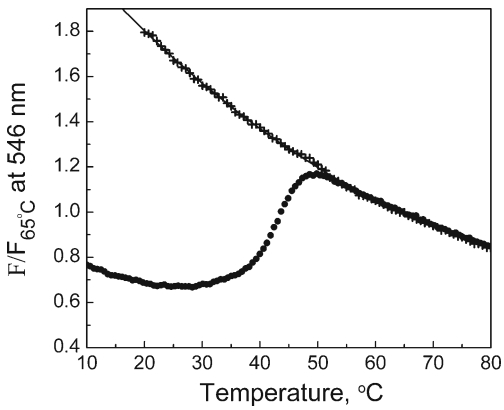

Fig. 6 Temperature dependencies of the (dT)$_{15}$Pzn (+) and poly(dA)·(dT)$_{15}$Pzn (●) fluorescence intensity normalized by their own values at 65 °C. Third order polynomial fit to the (dT)$_{15}$Pzn fluorescent melting curve is represented by the solid line. Fluorescence was registered under 545 nm, λ_{exc}=450 nm. Other conditions are as in the legend to Fig. 5

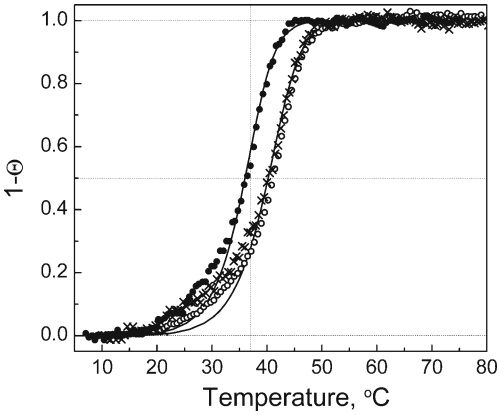

Fig. 7 Helix-to-coil transitions of poly(dA)·(dT)$_{15}$ (●) and poly(dA)·(dT)$_{15}$Pzn (+, ○) duplexes in the presence of 0.1 M NaCl. Symbols (+) correspond to the absorption data, (○) – to the fluorescence data. Solid lines represent the best fits to the experimental data obtained using Eq. 5 of two-state model

state, $\Theta(t)$, can be calculated from the equation for total fluorescence intensity of the sample [21]:

$$F = F_f(1-\Theta) + F_d\Theta \tag{3}$$

In such a way:

$$\Theta(t) = \frac{F_f - F}{F_f - F_d} = \frac{1 - \frac{F}{F_f}}{1 - \frac{F_d}{F_f}} \tag{4}$$

where F_f and F_d are fluorescence intensities of (dT)$_{15}$Pzn in the free state and bond to poly(dA) correspondingly (Fig. 6). Values of the temperature dependent F_f were taken from third order polynomial fit to the experimentally obtained fluorescent melting profile for the free (dT)$_{15}$Pzn.

As seen in Fig. 7, the transition curve constructed from poly(dA)·(dT)$_{15}$Pzn fluorescence melting data is somewhat shifted toward the higher temperatures relatively to the absorption one. Helix-to-coil transition midpoint temperature determined from fluorescent data is 0.8 °C higher than that obtained from absorption ones. This shift can be explained by the fact that absorption and fluorescence melting curves monitors the different processes occurring in the sample: the first one reflects the separation of dA·dT-base pairs, whereas the second one corresponds to the chromophore release. Since intercalation sites are the most stable, they presumably melt after the AT-pairs separations. In such a way, the fluorescent melting curve describes the completion of the duplex dissociation. Thus, it is more correct to determine the thermodynamic parameters of helix-to-coil transition from absorption melting data.

To evaluate the thermodynamic parameters of these transitions, the experimental transition curves were fitted to the

equation based on all-or-none binding model [33] (solid lines in Fig. 7):

$$\ln\frac{\Theta}{(1-\Theta)^2 C} = \frac{\Delta S}{R} - \frac{\Delta H}{RT} \quad (5)$$

where C is the total molar concentration of $(dT)_{15}$ or $(dT)_{15}$Pzn strands. Taking into a consideration the possibility of triplex formation [34], this procedure was performed in such a way that achieved the best fits of the high-temperature part of transition data. The obtained changes in the standard enthalpy, entropy, and Gibbs free energy at 37 °C are summarized in Table 2 along with the transition midpoint temperatures. As it is known [35], a binding of both a short unmodified oligothymidylate and its conjugate with intercalative dye to long complementary polynucleotide chain has cooperative character. Consequently, the determined thermodynamic parameters represent a combination of those for proper oligonucleotide binding to an isolated complementary site and those corresponding to the interaction between neighboring oligonucleotides [36].

Discussion

As expected, an attachment of phenazine derivative to the 5′-end of pentadecathymidilate strengthens the binding affinity of the $(dT)_{15}$Pzn conjugate for poly(dA) in comparison with unmodified oligonucleotide. Concomitant Pzn-induced increase in the helix-to-coil transition midpoint temperature, ΔT_m, of about 4.5 °C was registered. This value is comparable with that reported for acridine-linked oligonucleotide of the similar length. For example, upon the binding of $d(TTTAA)_3$ oligonucleotide 3′-end modified by acridine derivative to complementary sequence $(AAAUU)_3$ the increase of duplex melting temperature, ΔT_m=4.0 °C, was found [37]. Supposed mechanism of the binding enhancement by Pzn consists in the intercalation of planar imidazophenazine molecule into the duplex structure formed by the conjugate with the complementary poly(dA) strand. In this case π-stacking of the chromophore with adenine bases occurs. The 2.5-fold quenching of Pzn fluorescence, spectral shifts of the absorption and fluorescence bands, and the 9 % hypochromism in the visible absorption band argue in support of this point of view.

Estimation of the thermodynamic parameters of duplex formation using simple two-state model (Table 2) shows that the negative changes in transition enthalpy, ΔH, and entropy, ΔS, for unmodified poly(dA)·$(dT)_{15}$ calculated per oligonucleotide strand are equal to 99 kcal/mol and 295.3 cal/mol·K correspondingly, that gives the change in standard Gibbs free energy, ΔG, calculated at 37 °C of about −7.4 kcal/mol. A value of the duplex formation enthalpy, −6.6 kcal/mol per base pairs, calculated in our study is in good agreement with −6.8 kcal/mol per base pairs obtained in [34] for poly(dA)·$(dT)_8$ under similar ionic condition by the concentration variation method. The T_m value for poly(dA)·$(dT)_{15}$ duplex obtained in our study is 4.5 °C lower then that reported in [27] for the same system (36 and 40.5 °C, respectively). The difference can be explained by higher ionic strength of the buffered solutions used in [27], where the experimental study was performed in 0.015 M trisodium citrate buffer with 0.15 M NaCl, as well as by the difference in polymer concentration (unfortunately, it was not clearly indicated in that work). Taking into account that the polynucleotide duplex melting temperature is linearly dependent on lg$I$, where I is the monovalent ion concentration in the buffered solution (in our case – sodium ions), as well as the linearly dependencies of $1/T_m$ on lg$C$ and $1/m$ [27, 33, 38], where C is oligomer concentration, m – oligonucleotide length, we can conclude that our data is in good agreement with the values reported in [27].

As it is seen from the Table 2, the end-modification of $(dT)_{15}$ oligonucleotide by the intercalative phenazine derivative results in less negative changes in both transition enthalpy (by 6 kcal/mol) and entropy (by 23.5 cal/mol·K) upon the duplex formation with deoxypolynucleotide poly(dA). Such effect is opposite to that usually observed for the similar complexes formed between a dye-modified oligothymidilate and ribopolynucleotide poly(rA) [11, 21], where more negative values of ΔH and ΔS are realized in comparison with those obtained for the unmodified counterpart. However in spite of the less change in ΔH value

Table 2 Thermodynamic parameters of the duplex formation for $(dT)_{15}$ and $(dT)_{15}$Pzn with poly(dA) in 2.5 mM cacodylate buffer (pH 6.9) with 0.5 mM EDTA in the presence of 0.1 M NaCl. Adenine-to-thymine ratio was 1:1 in the samples; the poly(dA) concentration was 100 μM in the nucleic bases

Compound	Method	T_m (°C)	-ΔH (kcal/mol)	-ΔS (cal/mol·K)	-ΔG[a] (kcal/mol)	K_{eq}[a] (M^{-1})
poly(dA)·$(dT)_{15}$	Abs. melt.	36.0	99	295.3	7.4	$1.64\cdot10^5$
poly(dA)·$(dT)_{15}$Pzn	Abs. melt.	40.2	93	271.8	8.7	$1.35\cdot10^6$
poly(dA)·$(dT)_{15}$Pzn	Flu. melt.	41.0	–	–	–	–

[a] Calculated at t=37 °C using equation $\Delta G = \Delta H - T\Delta S$

obtained for poly(dA)·$(dT)_{15}$ under Pzn attachment a thermostability of the duplex is not reduced as a results of the entropy compensation effect. Entropy contribution to the binding free energy turns out to be larger than enthalpy one that gives the stabilizing increment in ΔG of 1.3 kcal/mol per oligonucleotide strand or 0.087 kcal/mole per AT-pair. Such ΔH and ΔS behavior obtained for helix-to-coil transition in poly(dA)·$(dT)_{15}$ Pzn system can be explained by "aberrant" thermodynamics of dyes binding to the poly(dA)·poly(dT) found in the work [39] where it was shown that the dye complexation is strongly driven by a large positive entropy change despite of a weak enthalpy of binding. The additional favorable contribution to the binding free energy corresponds to more than 8-fold rise of the equilibrium binding constant calculated under the physiological temperature of 37 °C using formula: $\frac{K_2}{K_1} = e^{-\frac{\Delta G_2 - \Delta G_1}{RT}}$, where K_1 and K_2 are the binding constants for poly(dA)·$(dT)_{15}$ and poly(dA)·$(dT)_{15}$Pzn duplexes accordingly. It should be noted that the value of the ΔG increment obtained in the present study for poly(dA)·$(dT)_{15}$Pzn system where Pzn was tethered to the 5′-end of pentadecathymidylate via flexible linker (1.3 kcal/mol) is somewhat lower than those obtained earlier under similar experimental conditions for $(dA)_{15}$·$(dT)_{10}$PznRib (1.5 kcal/mol) [20] and poly(rA)·$(dT)_{14}$PznRib (1.4 kcal/mol) [22] duplexes where Pzn nucleoside analogue was introduced directly at the 3′-end of oligonucleotide. It can be explained both by the difference in the chromophore mobility observed in these two cases and by the typically greater stabilizing effect observed for 3′-end modification in comparison with 5′-end ones [40] (see below). So, a Pzn chromophore attached to the oligonucleotide end via the flexible linker has much more degree of freedom in comparison with the quite rigid nucleoside analogue that leads to worse overlapping between the π-electronic systems and displays a lesser fluorescence quenching. The attachment of Pzn nucleoside guarantees a predetermined position of the chromophore in duplex and provides greater stabilization effect than that of a flexibly linked dye. But a multi-step procedure of its chemical synthesis is much more difficult. The method of post-synthetic oligonucleotide end modification with various molecules via suitable linkers is widely used, in part because of relatively simple synthetic procedure. The length and the chemical structure of the linker strongly influence the binding cooperativity of the intercalators conjugated to oligonucleotide end [41]. It was demonstrated that a more favorable linker consists of 5–6 carbon atoms. Hexamethylene linker was chosen in our study for the dye attachment.

Unfortunately, the available thermodynamic data related to the binding of synthetic oligonucleotides modified by intercalative dye are very limited and correspond to the oligonucleotides of different length and base composition. A direct comparison and an analysis are also complicated because in most cases an effect of the intercalator tethered to the oligonucleotide on the stability of its complex with complementary target is evaluated by comparing the corresponding melting temperatures for modified and unmodified systems. The data on the changes in the thermodynamic parameters like enthalpy, entropy, Gibbs free energy was considered only in rare cases. However, T_m value depends not only on the intercalator properties but also on the oligonucleotide base composition and length, type and length of complementary biopolymer, oligonucleotide concentration, concentration of counterions in the solution, type and length of the linker, place of the dye attachment to the oligomer etc. Since an additional favorable contribution to the total binding energy caused by the oligonucleotide modification decreases with the increase of oligonucleotide length, then the relative effect of the intercalator attachment on the duplex formation is more pronounced for shorter oligonucleotide that induces stronger increase in corresponding T_m value. For example, the melting temperature increment measured under similar experimental condition for duplex poly(rA)·$(dT)_n$ and conditioned by the covalent attachment of acridine dye to 3′-end of the oligonucleotide via pentamethylene linker is amounted to more than 29 °C for n=4; 23.2 °C for n=8 and 13.8 °C for n=12 [35]. Also, for the complexes formed by the $(dT)_n$–intercalator conjugates of the same length with complementary oligo- or polyribonucleotide a stabilization effect is more pronounced than in the case of complementary deoxyribopolymers. Such behavior can be explained if we take into account well-known fact that dA·dT base pairs are more stable than rA·dT ones, thus equal additional energy contribution due to oligonucleotide modification will induce more considerable changes in the less stable system. For example, for duplexes formed by Acr-$(dT)_8$ conjugate with poly(dA) and poly(rA) the T_m changes resulted from the acridine dye attachment are 16.4 and 20.3 °C correspondingly in the case of 3′-end modification, whereas for 5′-end modification the values of 8.3 and 12.4 °C were registered [40]. From above data it is also seen that 3′-end modification turned out to be more efficient in terms of stabilization as compared to 5′-conjugation. Thus a comparison between only T_m changes induced by intercalators is appropriate in the case of the systems where base composition and length of oligonucleotides, their concentration in the solution as well as ionic conditions are the same, while the chromophore type, linker length or conjugation site undergoes some changes. In the same time, a comparison between the corresponding changes in the thermodynamic characteristics of unmodified and modified systems, e.g. in change of Gibbs free energy calculated under physiological temperature of 37 °C, can

characterize just a contribution of the intercalator to the complex stability, putting aside the abovementioned intrinsic parameters of the system studied.

Conclusions

The attachment of the imidazophenazine derivative to the 5′-terminus of pentadecathymidylate via flexible linker enhances the stability of its duplex formed with poly(dA) increasing the helix-to-coil transition midpoint temperature by 4.5 °C, and gives 1.3 kcal/mol increment in standard Gibbs free energy at 37 °C per oligonucleotide strand. The stabilizing effect produced by the neutral imidazophenazine is comparable with that known for cationic intercalating dyes (for example, acridine derivatives) conjugated to oligonucleotide by the similar chemistry. The data obtained can be included in the thermodynamic database for normal and modified nucleic acids (NTDB) (http://ntdb.chem.cuhk.edu.hk).

References

1. Riordan ML, Martin JC (1991) Oligonucleotide-based therapeutics. Nature 350:442–443
2. Cook PD (1991) Medicinal chemistry of antisense oligonucleotides – future opportunities. Anti Canc Drug Des 6:585–607
3. Dean NM, Bennett CF (2003) Antisense oligonucleotide-based therapeutics for cancer. Oncogene 22:9087–9096
4. Bennett CF, Cowsert LM (1999) Antisense oligonucleotides as a tool for gene functionalization and target validation. Biochim Biophys Acta 1489:19–30
5. Dias N, Stein CA (2002) Antisense oligonucleotides: basic concepts and mechanisms. Mol Cancer Ther l:347–355
6. Aboul-Fadl T (2005) Antisense oligonucleotides: the state of the art. Curr Med Chem 12:2193–2214
7. Milligan JF, Matteucci MD, Martin JC (1993) Current concepts in antisense drug design. J Med Chem 36:1923–1937
8. Helene C, Toulme J (1990) Specific regulation of gene expression by antisense, sense and antigene nucleic acids. Biochim Biophys Acta 1049:99–125
9. Toulmé JJ, Dausse E, Santamaria F, Rayner B (2002) Aptamers for controlling gene expression. In: Mahato R (ed) Pharmaceutical approaches to nucleic acid-based therapeutics. Taylor and Francis, London, pp 89–120
10. Letsinger RL, Schott ME (1981) Selectivity in binding a phenanthridinium dinucleotide derivative to homopolynucleotides. J Am Chem Soc 103:7394–7396
11. Asseline U, Delarue M, Lancelot G, Toulme F, Thuong NT, Montenay-Garestier T, Helene C (1984) Nucleic acid binding molecules with high affinity and base sequence specificity: intercalating agents covalently linked to oligodeoxynucleotides. Proc Natl Acad Sci USA 81:3297–3301
12. Dubey IY (2006) Oligonucleotide conjugates with intercalating agents: synthesis and biological activity. Ukr Bioorg Acta 4:42–59
13. Da Ros T, Spalluto G, Prato M, Saison-Behmoaras T, Boutorine A, Cacciari B (2005) Oligonucleotides and oligonucleotide conjugates: a new approach for cancer treatment. Curr Med Chem 12:71–88
14. Makitruk VL, Yarmoluk SN, Shalamay AS, Alexeeva IV (1991) Oligonucleotides modified with phenazine derivatives. Nucl Ac Symp Ser 24:244
15. Shaw JP, Kent K, Bird J, Fishback J, Froehler B (1991) Modified deoxyoligonucleotides stable to exonuclease degradation in serum. Nucl Ac Res 19:747–750
16. Zamaratski E, Chattopadhyaya J (1998) Synthesis of phenazine-tethered arabino and xylofuranosyl ologonucleotide conjugates: the thermal stability and fluorescence properties of their duplexes (DNA-DNA & DNA-RNA) & triplexes. Tetrahedron 54:8183–8206
17. Nurmukhametov RN (1971) Absorption and fluorescence of aromatic compounds. Chemistry, Moscow, USSR. (in Russian)
18. Ryazanova OA, Zozulya VN, Voloshin IM, Karachevtsev VA, Makitruk VL, Stepanian SG (2004) Absorption and fluorescent spectral studies of imidazophenazine derivatives. Spectrochim Acta A Mol Biomol Spectrosc 60:2005–2011
19. Ryazanova OA, Voloshin IM, Makitruk VL, Zozulya VN, Karachevtsev VA (2007) pH – Induced changes in electronic absorption and fluorescence spectra of phenazine derivatives. Spectrochim Acta A Mol Biomol Spectrosc 66:849–859
20. Zozulya V, Blagoi Yu, Dubey I, Fedoryak D, Makitruk V, Ryazanova O, Shcherbakova A (2003) Anchorage of an oligonucleotide hybridization by a tethered phenazine nucleoside analogue. Biopolymers (Biospectroscopy) 72:264–273
21. Zozulya V, Scherbakova A, Dubey I (2000) Calculating helix-to-coil transitions of duplexes formed by phenazine-conjugated oligonucleotide using fluorescence melting data. J Fluoresc 10:49–53
22. Ryazanova OA, Dubey IY, Zozulya VN (2008) Investigation of the effect of covalently attached phenazine dye on helix-to-coil transition in mixed poly(rA)-$(dT)_{14}$ system. Biophysical Bulletin 20:17–23
23. Wachter L, Jablonski J, Ramachandran KL (1986) A simple and efficient procedure for the synthesis of 5′-aminoalkyl oligodeoxyoligonucleotides. Nucl Ac Res 14:7985–7994
24. Dubey IY, Fedoryak DM (2006) Novel reagents for oligonucleotide labeling with imidazophenazine. Ukr Bioorg Acta 4:3–9
25. Dubey I, Pratviel G, Meunier B (1998) Modification of the thiourea linkage of fluorescein-oligonucleotide conjugate to a guanidinium motif during ammonia deprotection. Bioconj Chem 9:627–632
26. Chalikian TV, Völker J, Plum GE, Breslauer KJ (1999) A more unified picture for the thermodynamics of nucleic acid duplex melting: A characteriztion by calorimetric and volumetric techniques. Proc Natl Acad Sci USA 96:7853–7858
27. Cassani G, Bollum FJ (1969) Oligodeoxythymidylate: polydeoxyadenylate and oligodeoxyadenylate: polydeoxythymidylate interactions. Biochemistry 8:3928–3936
28. Zozulya VN, Ryazanova OA, Voloshin IM, Glamazda AYu, Karachevtsev VA (2010) Spectroscopic detection of tetracationic porphyrin H-aggregation on polyanionic matrix of inorganic polyphosphate. J Fluoresc 20:695–702
29. Lakowicz JR (2006) Principles of fluorescence spectroscopy. Springer, NY
30. Porumb H (1978) The solution spectroscopy of drugs and the drug-nucleic acid interactions. Prog Biophys Mol Biol 34(3):175–195
31. Kibler-Herzog L, Kell B, Zon G, Shinozuka K, Mizan S, Wilson D (1990) Sequence dependent effects in methylphosphonate deoxyribonucleotide double and triple helical complexes. Nucleic Acids Res 18:3545–3555
32. Löber G, Kittler L (1978) Redox mechanism involved in the fluorescence quenching of dyes bound to deoxyribonucleic acid (DNA). Stud Biophys 73:25–30
33. Marky LA, Breslauer KJ (1987) Calculating thermodynamic data for transitions of any molecularity from equilibrium melting curves. Biopolymers 26:1601–1620

34. Pless RC, Ts'o POP (1977) Duplex formation of a nonionic oligo (deoxythymidylate) analog [heptadeoxythymidylyl-(3′-5′)-deoxythymidine heptaethyl ester (d-[Tp(Et)]$_7$T)] with poly(deoxyadenylate). Evaluation of the electrostatic interaction. Biochemistry 16:1239–1250
35. Asseline U, Delarue M, Lancelot G, Toulme F, Thuong NT, Montenay-Garestier T, Helene C (1984) Nucleic acid binding molecules with high affinity and base sequence specificity: intercalating agents covalently linked to oligodeoxynucleotides. Proc Natl Acad Sci USA 81:3297–3301
36. Springgate MW, Poland D (1973) Cooperative and thermodynamic parameters for oligoinosinate-polycytidylate complexes. Biopolymers 12:2241–2260
37. Toulme JJ, Krisch HM, Loreau N, Thuong NY, Helene C (1986) Specific inhibition of mRNA translation by complementary oligonucleotides covalently linked to intercalating agents. Proc Natl Acad Sci USA 83:1227–1231
38. Porschke D (1971) Cooperative nonenzymic base recognition. II. Thermodynamics of the helix coil transition of oligoadenylic + oligouridylic acids. Biopolymers 10:1989–2013
39. Breslauer KJ, Remeta DP, Chou W-Y, Ferrante R, Curry J, Zaunczkowski D, Snyder JG, Marky LA (1987) Enthalpy-entropy compensations in drug-DNA binding studies. Proc Natl Acad Sci USA 84:8922–8926
40. Tuong NT, Asseline U, Roig V, Takasugi M, Helene C (1987) Oligo(α-deoxynucleotide)s covalently linked to intercalating agents: differential binding to ribo- and deoxyribopolynucleotides and stability towards nuclease digestion. Proc Natl Acad Sci USA 84:5129–5133
41. Orson FM, Kinsey BM, McShan WM (1994) Linkage structures strongly influence the binding cooperativity of DNA intercalators conjugated to triplex forming oligonucleotides. Nucleic Acids Res 22:479–484